Colloid Polym Sci 278:821–829 (2000)

ORIGINAL CONTRIBUTION

C. S. Chern
C. W. Liu

Microemulsion polymerization of styrene stabilized by sodium dodecyl sulfate and diethylene glycol monoalkyl ether

Received: 24 December 1999
Accepted: 9 February 2000

C. S. Chern (✉) · C. W. Liu
Department of Chemical Engineering
National Taiwan University of Science and Technology
43 Keelung Road, Section 4
Taipei 106, Taiwan
e-mail: chern@ch.ntust.edu.tw
Fax: +886-2-27376644

Abstract The effects of the cosurfactants diethylene glycol monoalkyl ether [$C_iH_{2i+1}O(CH_2CH_2O)_jOH$ (C_iE_j; $i = 4$, 6 and $j = 1$, 2)] on the formation of an oil-in-water styrene (ST) microemulsion and the subsequent free radical polymerization were studied. For comparison, the data for the $C_iH_{2i+1}OH$ (C_iOH; $i = 4$, 6) systems obtained from the literature were also included in this work. Sodium dodecyl sulfate was used as the surfactant. The pseudo three-component phase diagram (macroemulsion, microemulsion and lamellar gel phases) was constructed for each cosurfactant. The primary parameters selected for the polymerization study are the concentrations of cosurfactant and styrene. The number of latex particles nucleated is much smaller than that of the microemulsion droplets initially present in the reaction system. Limited flocculation of the latex particles occurs to some extent during polymerization. Among the cosurfactants investigated, the C_4OH-containing polymerization system is the least stable. By contrast, the diethylene glycol monoalkyl ether group of C_iE_j tends to enhance the latex stability. C_iE_j is more effective in stabilizing the ST microemulsion and the subsequent polymerization in comparison with the C_iOH counterpart.

Key words Microemulsion polymerization · Styrene · Sodium dodecyl sulfate · Diethylene glycol monoalkyl ether

Introduction

Thermodynamically stable oil-in-water (O/W) microemulsions consist of oil droplets (1–10 nm in diameter) dispersed in water. Such a transparent colloidal system can be stabilized by surfactant (e.g., sodium dodecyl sulfate, SDS) and cosurfactant (e.g., short-chain alcohols). Incorporation of cosurfactant into the adsorbed layer of SDS around the droplet greatly decreases the electrostatic repulsion between two SDS molecules, minimizes the oil–water interfacial tension and reduces the persistence length of the interfacial layer (i.e., enhances the flexibility of the interfacial membrane). All these synergistic factors promote the spontaneous formation of transparent one-phase microemulsions [1]. If a vinyl monomer (e.g., styrene, ST) is chosen as the major component of the dispersed phase, stable colloidal particles comprising only a few high-molecular-weight polystyrene (PST) chains are produced via free-radical polymerization (termed microemulsion polymerization) [2–10]. In our previous study [11], the influence of the alkyl chain length of alcohols [1-butanol (C_4OH), 1-pentanol (C_5OH) and 1-hexanol (C_6OH)] on the formation of ST microemulsions and the subsequent polymerization inside the monomer droplets was studied. The objective of this work was to study the role of two series of cosurfactants [series 1: C_4OH, ethylene glycol monobutyl ether (C_4E_1) and diethylene glycol monobutyl ether (C_4E_2); series 2: C_6OH, ethylene glycol monohexyl ether (C_6E_1) and diethylene glycol mono-

hexyl ether (C_6E_2)] in the ST microemulsion polymerization using SDS as the surfactant and sodium persulfate as the initiator. For comparison, the data for the C_iOH ($i = 4$, 6) system obtained from Ref. [11] were also included in this work. Variation of the hydrophobic tail (butyl versus hexyl) or the hydrophilic head (hydroxyl, ethylene glycol or diethylene glycol) of the cosurfactants changes their partition among the oily, interfacial and aqueous phases. This should have an impact on the SDS/(C_iOH or C_iE_j) ($i = 4$, 6 and $j = 1$, 2) stabilized polymerizations.

Experimental

Materials

The materials used were ST (Taiwan Styrene Co.), SDS (J. T. Baker), CH_3OH (Acros), C_4E_1 (Janssen Chimica), C_4E_2 (Acros), C_6E_1 (Wako), C_6E_2 (Aldrich), $Na_2S_2O_8$ (Riedel-de-Haen), $NaHCO_3$ (buffer) (Janssen Chimica), tris(hydroxymethyl)aminomethane (Acros), nitrogen (Ching-Feng-Harng Co.) and deionized water (Barnsted Nanopure Ultrapure Water System, specific conductance below 0.057 μS/cm). ST was distilled under reduced pressure before use. All other chemicals were used as received.

Preparation of the microemulsion

The cosurfactant was added successively to the milky macroemulsion comprising water, SDS and ST with mild mixing at room temperature. The transitions from the milky macroemulsion to the transparent microemulsion and then to the lamellar gel phase were observed visually. By changing the amount of ST in the initial macroemulsion and repeating the cosurfactant titration procedure, the pseudo three-component phase diagram was constructed. The microemulsion region identified in this manner was verified by independent measurements of viscosity (η) (Brookfield LVT) and conductivity (κ) (Orion 115) [11].

Microemulsion polymerization

A typical recipe consists of 25 g water, 2.75 g (381 mM) SDS, 0.4 g (109 mM) C_6E_1, 1.2 g ST, 0.5 mM $Na_2S_2O_8$ and 0.1 mM $NaHCO_3$, in which the molar concentration is based on total water. Before the start of polymerization, the reaction medium was purged with N_2 for 20 min. Polymerization was carried out in a 100-ml reactor at 70 °C for 8 h. The latex product was filtered through a 200-mesh (0.074-mm) screen to collect the filterable solids. The latex particle diameter (d_p) was measured by dynamic light scattering (Otsuka Photal LPA 3000/3100). The reported d_p data represent the average of at least seven measurements. The zeta potential (ζ) of the latex particles was determined using a Malvern Zetamaster. The pH 7 tris(hydroxymethyl)aminomethane buffer (20 mM) was used as the dilution solution for the latex sample [latex/buffer = 1/5 (v/v)]. The reported ζ data represent the average of at least ten measurements. The latex particles were precipitated by an excess of methanol, followed by thorough washes with methanol and water to remove residual SDS, C_6E_1 and other impurities. The conversion (X) was then determined by the gravimetric method. The molecular weight of PST was determined by gel permeation chromatography (Waters).

Results and discussion

Formation of O/W microemulsion

The pseudo three-component phase diagram for the SDS/(C_iOH or C_iE_j)-stabilized ST microemulsions is shown in Fig. 1. The fact that a gel phase was not observed for the C_4OH- or C_4E_j-containing system within the composition range studied implies that the formation of a gel phase is suppressed when the hydrophilicity of the cosurfactants is high enough (Fig. 1a). The range of the microemulsion region in decreasing order is $C_6OH < C_6E_1 < C_6E_2$ (Fig. 1b), which also correlates well with the hydrophilicity of the cosurfactants ($C_6OH < C_6E_1 < C_6E_2$); however,

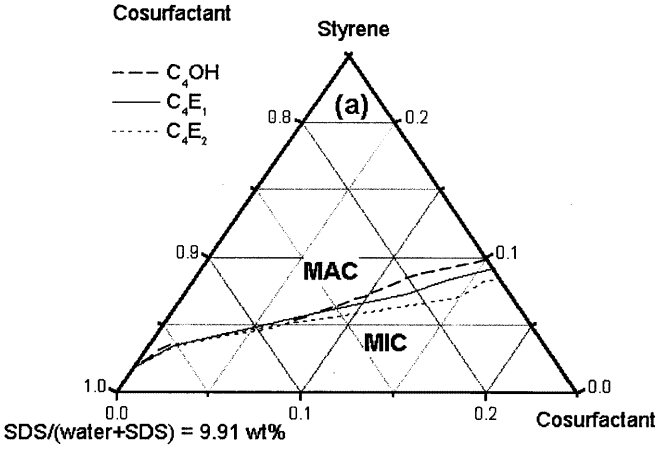

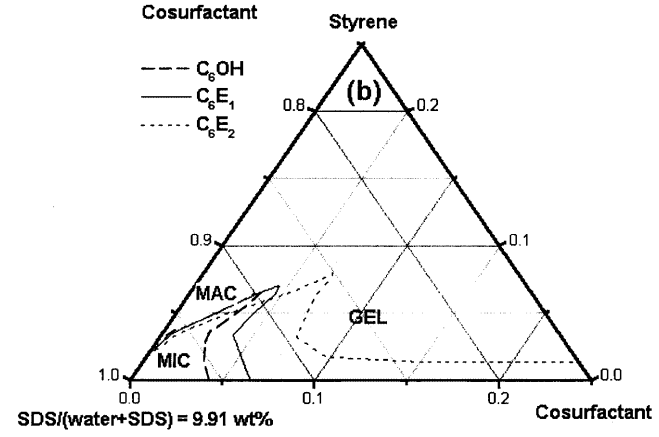

Fig. 1a, b Pseudo three-component phase diagram for the sodium dodecyl sulfate (*SDS*)/[$C_iH_{2i+1}OH$(C_iOH) or $C_iH_{2i+1}O(CH_2CH_2O)_j$ OH(C_iE_j)] stabilized styrene (ST) microemulsions. **a** C_4OH, C_4E_1, C_4E_2; **b** C_6OH, C_6E_1, C_6E_2: *MAC*, *MIC* and *GEL* represent milky macroemulsion, transparent microemulsion and lamellar gel phase, respectively

this trend diminishes for the microemulsions with C_4OH and C_4E_j because all these cosurfactants have a quite short butyl tail and they are relatively water-soluble. The value of the hydrophile–lipophile balance (HLB) for C_4OH, C_4E_1, C_4E_2, C_6OH, C_6E_1 and C_6E_2 estimated by the group contribution method [12] is 7, 7.33, 7.66, 6.05, 6.38 and 6.71, respectively. These HLB data suggest that the difference in the surface activity of C_iOH and C_iE_j is responsible for the quite different cosurfactant performance between the series of C_4OH and C_4E_j and the series of C_6OH and C_6E_j. It is interesting to note that the gel phase is also absent from the C_6E_2 system provided that the ST content is low enough. This is because the HLB value of C_6E_2 is 6.71, which is quite close to the values of C_4OH and C_4E_j.

Figures 2 and 3 show the η and κ versus C_iE_2 concentration data, respectively, for the recipe containing 25 g water, 381 mM SDS and 569 mM ST. The C_iOH system also shows similar η and κ profiles to those of the C_iE_2 system [11]. For the C_6E_2 system, η remains relatively constant when the macroemulsion is transformed into a microemulsion. This is followed by a rapid increase in η when the transition from the microemulsion to the lamellar gel phase occurs (Fig. 2b). κ first increases to a maximum when the C_6E_2 concentration increases from 0 to 390 mM (Fig. 3b). The increased κ is attributed to the reduced oil droplet size (i.e., the enhanced mobility of droplets). The higher the mobility of the negatively charged droplets, the higher the conductivity of the macroemulsion or microemulsion [13]. Immediately after the formation of the lamellar gel phase, κ starts to drop sharply. This is simply due to the fact that the η of the lamellar gel phase becomes very high and the mobility of the ions within the structured gel phase is greatly retarded as the C_6E_2 concentration is further increased.

For the C_4E_2 system, the η of the macroemulsion first increases with increasing C_4E_2 concentration (Fig. 2a). Immediately after the transition from the macroemulsion to a microemulsion, η decreases gradually upon further addition of C_4E_2. The initial increase in η is due to the following two competitive factors. First, the fraction of the relatively hydrophilic C_4E_2 in water cannot be ignored and, therefore, the volume fraction of the aqueous phase increases with increasing C_4E_2 concentration. This dilution effect reduces the η of the macroemulsion. In contrast, the oil droplets become smaller (or the number of droplets increases) as more C_4E_2 is incorporated into the droplet surface layer. The interactions among these droplets are greatly enhanced, thereby leading to the increased resistance toward the applied shear force. It is then postulated that the latter effect overrides the former and, therefore, η increases with increasing C_4E_2 concentration ($0 \rightarrow 390$ mM). When the C_4E_2 concentration exceeds 390 mM, the rate of change in the microemulsion droplet size with C_4E_2 concentration is greatly reduced. Thus, the dilution effect becomes more important and η starts to decrease with increasing C_4E_2 concentration. Just like the C_6E_2 system, the κ of the macroemulsion increases with increasing C_4E_2 concentration. It is interesting to note that the κ of the microemulsion decreases with increasing C_4E_2 concentration (Fig. 3a). This trend is caused by the previously mentioned dilution effect in combination

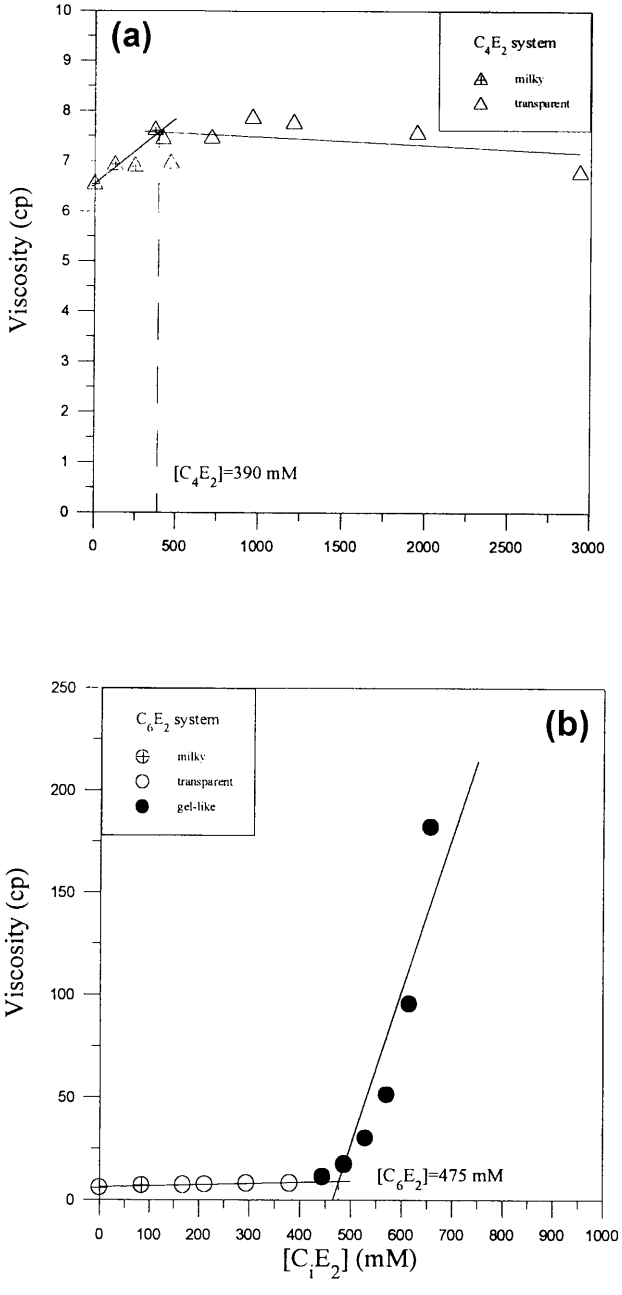

Fig. 2a, b Viscosity as a function of the cosurfactant concentration for the recipe containing 25 g water, 381 mM SDS and 569 mM ST. **a** C_4E_2 and **b** C_6E_2

with the decreased dielectric constant of the aqueous solution. Figures 2 and 3 show that both η and κ are sensitive to changes in the colloidal structure, except for the transition from the macroemulsion to a microemulsion for the C_6E_2 sample monitored by viscosity measurement. The data of the molar ratio of cosurfactant to SDS at the point where the transition from the macroemulsion to a microemulsion (or from the microemulsion to a lamellar gel phase) occurs, determined by the naked eye and measurements of η and κ, are consistent with one another (Table 1).

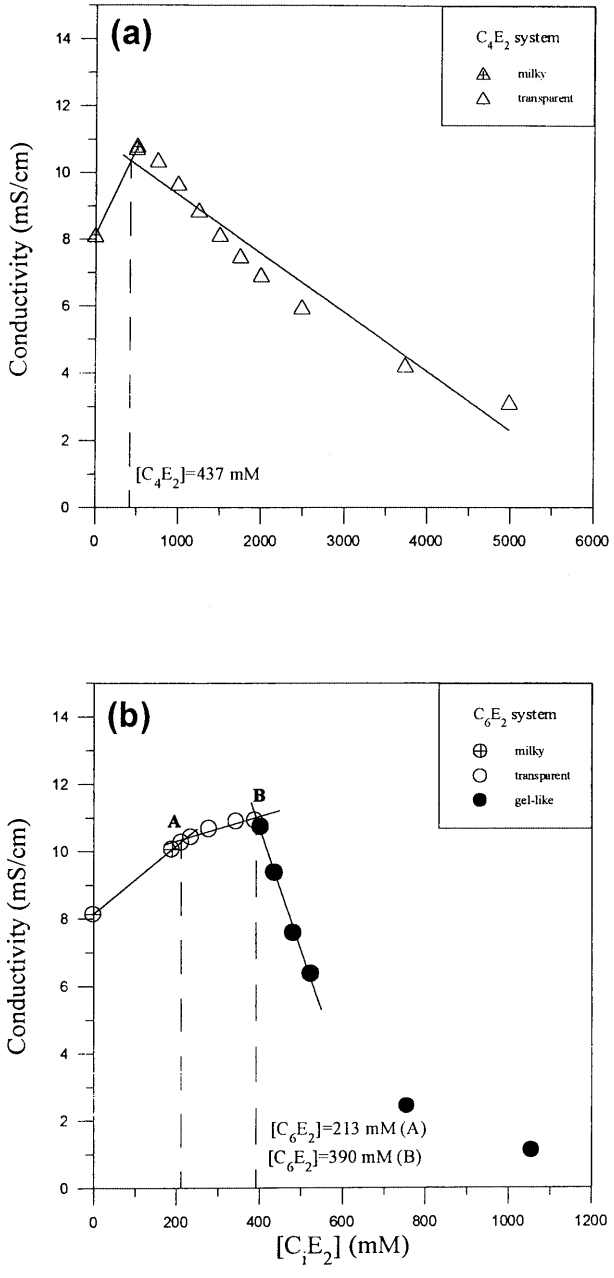

Fig. 3a, b Conductivity as a function of the cosurfactant concentration for the recipe containing 25 g water, 381 mM SDS and 569 mM ST. **a** C_4E_2 and **b** C_6E_2

The molar ratios of all the added C_4OH, C_4E_1, C_4E_2, C_6OH, C_6E_1 and C_6E_2 to SDS at the point where the transition from the macroemulsion to a microemulsion occurs ($R_{mac/mic}$) are about 2.7, 1.4, 1.8, 0.7, 0.4 and 0.5, respectively (Table 1). This result suggests that it is more efficient for C_6OH (or C_6E_j) to adsorb onto the droplet surface layer in comparison with the C_4OH (or C_4E_j) counterpart. In addition to the oil–water interface, a significant fraction of C_4OH (or C_4E_j) can partition into the aqueous phase due to its relatively hydrophilic nature. As a result, a much higher $R_{mac/mic}$ is achieved for the C_4OH (or C_4E_j) system. Furthermore, no gel phase is observed within the composition range studied for the C_4OH (or C_4E_j) system since more C_4OH (or C_4E_j) can be accommodated in the aqueous phase compared to the C_6OH (or C_6E_j) counterpart (Fig. 1). In summary, the performance of C_iOH and C_iE_j in stabilizing the ST microemulsions becomes insensitive to changes in the HLB of the cosurfactants when $7 < HLB < 7.7$ (Fig. 1a). On the other hand, the range of the microemulsion region increases significantly with increasing HLB for the C_iOH and C_iE_j systems with $6.1 < HLB < 6.7$ (Fig. 1b). Although C_4OH and C_4E_j show very similar phase behavior, $R_{mac/mic}$ in decreasing order is $C_4OH > C_4E_2 > C_4E_1$. This trend is achieved by the following two competitive factors. First, the bulky diethylene glycol group of the intercalated C_4E_j species is more effective in reducing the electrostatic repulsion between two surface SDS molecules in comparison with C_4OH and, therefore, promotes the formation of microemulsions. Nevertheless, C_4E_2 has a larger HLB than C_4E_1, thereby leading to a larger fraction of the initially added C_4E_2 in water. As a result, C_4E_1 exhibits the lowest $R_{mac/mic}$ among C_4OH and C_4E_j. That is, C_4E_1 is the optimum cosurfactant in

Table 1 Molar ratio of cosurfactant [1-butanol (C_4OH), ethylene glycol monobutyl ether (C_4E_1), diethylene glycol monobutyl ether (C_4E_2), 1-hexanol (C_6OH), ethylene glycol monohexyl ether (C_6E_1), diethylene glycol monohexyl ether (C_6E_2)] to sodium dodecyl sulfate (*SDS*) at the point at which the transition from macroemulsion (*MAC*) to microemulsion (*MIC*) or from MIC to lamellar gel phase (*GEL*) occurs (recipe = 25 g water + 381 mM SDS + 569 mM, styrene *ST*)

	C_4OH	C_4E_1	C_4E_2	C_6OH	C_6E_1	C_6E_2
MAC → MIC	2.66[a]	1.40[a]	1.08[a]	0.69[a]	0.43[a]	0.46[a]
	3.00[b]		1.02[b]			
	2.44[c]		1.15[c]	0.71[c]		0.56[c]
MIC → GEL	–	–	–	1.02[a]	–	1.26[a]
				1.16[b]		1.25[b]
				0.97[c]		1.02[c]

[a] Determined from the phase diagram
[b] Determined from viscosity
[c] Determined from conductivity

preparing the ST microemulsions. A similar trend ($R_{mac/mic}$: $C_6OH > C_6E_2 > C_6E_1$) is observed in the series of C_6OH and C_6E_j.

Microemulsion polymerization

The recipe and some experimental results obtained from the ST microemulsion polymerizations with various concentrations of C_iE_j are compiled in Tables 2–5 (C41-1–C41-4 in Table 2, C42-1–C42-4 in Table 3, C61-1–C61-4 in Table 4 and C61-1–C62-4 in Table 5). The effects of C_iOH and C_iE_j concentration on the diameter (d_p) and the number (N_p) of latex particles are shown in Figs. 4 and 5, respectively. In this series, the recipe comprises 25 g water, 381 mM SDS, 0.1 mM $NaHCO_3$, 577 mM ST for the C_4OH and C_4E_j systems (or 462 mM ST for the C_6OH and C_6E_j systems), 0.5 mM $Na_2S_2O_8$ and various levels of C_iOH and C_iE_j. It is shown that d_p increases (or N_p decreases) with increasing C_4OH concentration, whereas d_p (or N_p) is relatively insensitive to changes in C_6OH or C_iE_j concentration. The rapidly increased d_p with C_4OH concentration is due to the limited flocculation among the relatively unstable C_4OH-containing particles [11]. This is further supported by the largest total scrap data obtained from the C_4OH-stabilized latices. Figure 4a shows that the effectiveness of the cosurfactants in

Table 2 Recipe and some experimental results obtained from the ST microemulsion polymerization with C_4E_1 as the cosurfactant

	C41-1	C41-2	C41-3	C41-4	C41-5	C41-6	C41-7	C41-8
[C_4E_1] (%)	5.49	6.40	7.87	9.30	8.00	7.92	7.85	7.80
[ST] (%)	4.85	4.80	4.72	4.65	3.20	4.12	5.02	5.62
X (%)	96.7	94.8	95.1	97.3	90.1	96.5	97.3	93.2
$M_w \times 10^{-6}$ (g/mol)	3.66	3.05	2.93	2.59	2.15	2.40	2.66	3.36
Polydispersity index	3.33	2.73	1.85	2.85	3.05	2.14	2.25	1.59
No. of polystyrene chains per particle	6.4	7.9	9.0	13.0	8.4	9.5	10.1	8.6
ζ (mV)	−8.2	−7.6	−8.2	−10.4				
Total scrap $\times 10^3$ (%)	9.2	9.6	6.6	7.0	8.2	6.0	8.7	7.1

Table 3 Recipe and some experimental results obtained from the ST microemulsion polymerization with C_4E_2 as the cosurfactant

	C42-1	C42-2	C42-3	C42-4	C42-5	C42-6	C42-7	C42-8
[C_4E_2] (%)	5.49	6.40	7.87	9.30	8.00	7.92	7.85	7.80
[ST] (%)	4.85	4.80	4.72	4.65	3.20	4.12	5.02	5.62
X (%)	93.8	95.6	98.3	97.1	98.6	93.9	94.6	98.6
$M_w \times 10^{-6}$ (g/mol)	2.57	2.15	2.39	2.03	2.28	2.94	2.25	2.92
Polydispersity index	3.12	2.69	2.64	2.45	2.02	1.55	2.19	1.91
No. of polystyrene chains per particle	8.0	9.7	9.0	10.0	7.3	7.2	10.5	8.3
ζ (mV)	−6.3	−6.3	−5.5	−9.8				
Total scrap $\times 10^3$ (%)	9.0	8.4	7.8	7.4	7.8	7.3	7.5	7.6

Table 4 Recipe and some experimental results obtained from the ST microemulsion polymerization with C_6E_1 as the cosurfactant

	C61-1	C61-2	C61-3	C61-4	C61-5	C61-6	C61-7	C61-8
[C_6E_1] (%)	1.36	1.70	2.03	2.36	3.36	3.33	3.29	3.27
[ST] (%)	4.09	4.07	4.06	4.05	3.36	4.33	5.27	5.89
X (%)	86.1	89.6	87.4	90.7	92.3	90.9	96.9	94.5
$M_w \times 10^{-6}$ (g/mol)	3.20	2.96	2.76	3.09	3.15	3.33	3.14	3.53
Polydispersity index	2.00	2.22	1.97	1.93	1.87	2.06	1.76	1.69
No. of polystyrene chains per particle	5.9	6.6	7.6	7.2	5.8	6.1	7.4	7.4
ζ (mV)	−4.8	−4.3	−2.0	−4.2				
Total scrap $\times 10^3$ (%)	5.9	5.7	8.1	8.3	9.2	7.8	8.8	8.4

Table 5 Recipe and some experimental results obtained from the ST microemulsion polymerization with C_6E_2 as the cosurfactant

	C62-1	C62-2	C62-3	C62-4	C62-5	C62-6	C62-7	C62-8
$[C_6E_2]$ (%)	1.36	1.70	2.03	2.36	5.27	5.22	5.17	5.14
[ST] (%)	4.09	4.07	4.06	4.05	3.29	4.24	5.17	5.78
X (%)	97.2	98.1	95.3	96.6	96.4	96.3	98.1	98.7
$M_w \times 10^{-6}$ (g/mol)	2.60	2.71	2.75	2.76	2.70	2.53	3.65	3.80
Polydispersity index	2.01	1.80	2.29	2.07	1.90	2.04	2.70	1.58
No. of polystyrene chains per particle	6.3	7.0	7.5	7.5	6.8	8.7	6.6	6.6
ζ (mV)	−3.8	−4.3	−4.2	−14.4				
Total scrap $\times 10^3$ (%)	5.8	6.5	12.7	6.1	9.2	7.8	8.8	6.1

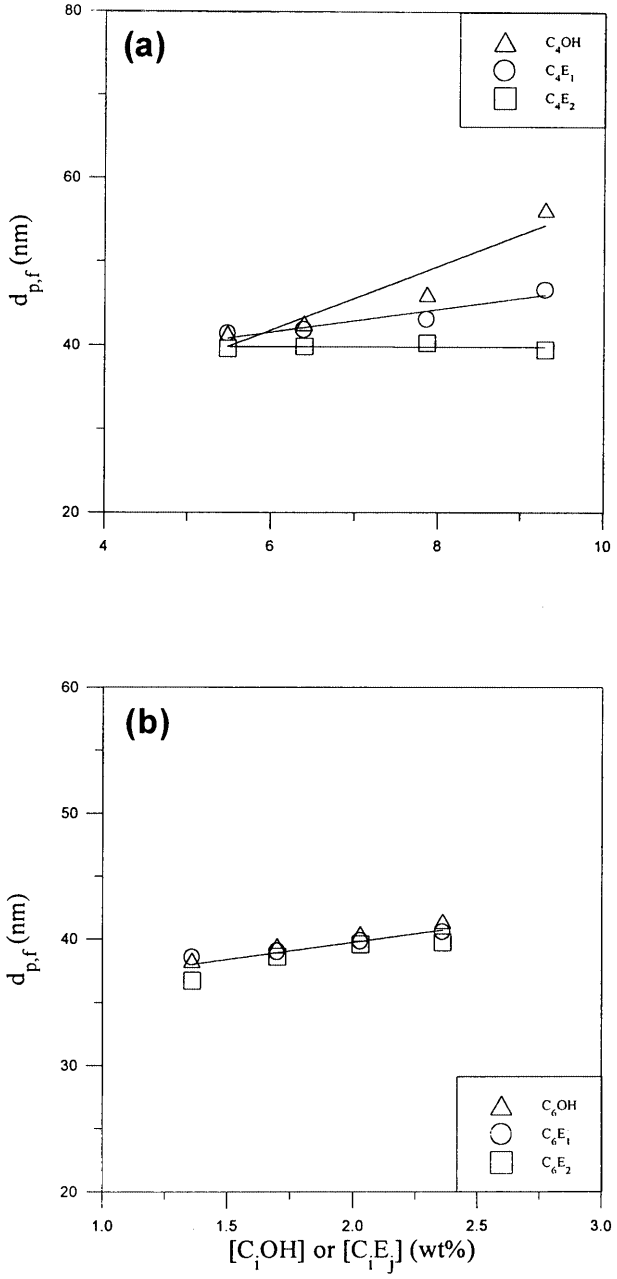

stabilizing the colloidal particles in decreasing order is $C_4E_2 > C_4E_1 > C_4OH$. The reason for this trend is not clear, but it is most likely related to the improved colloidal stability provided by the diethylene glycol monobutyl ether group of C_4E_j. As for the series of C_6OH and C_6E_j, the cosurfactants with a longer alkyl chain seem to perform equally well in stabilizing the microemulsion polymerization. In our previous work [11], we also showed that only a small fraction of the initial microemulsion droplets can be successfully nucleated. The remaining droplets then serve as a reservoir to provide the growing latex particles with ST, SDS and cosurfactant. This then results in a relatively large d_p (37–51 nm) compared to the microemulsion droplets (4 nm [14]). Another possible explanation is the limited flocculation of the latex particles due to the decreased compatibility between the cosurfactant and PST produced. This results in desorption of the cosurfactant out of the latex particle surface and, therefore, reduces the colloidal stability of the latex particles.

The polymer molecular weights obtained from the polymerizations with various levels of C_iOH and C_iE_j are very high, as shown by the weight-average molecular weight (M_w) and the polydispersity index (M_w/M_n, where M_n is the number-average molecular weight of PST) data in Ref. [11] and Tables 2–5, respectively. These data are also shown in Fig. 6a and b. The reciprocal of the number-average degree of polymerization ($1/X_n$) equals the chain transfer to monomer constant ($C_m = 4.5 \times 10^{-5}$ at 60 °C [15]) if each latex particle contains only one free radical until chain transfer to monomer occurs. The value of C_m at 70 °C should be larger than that at 60 °C and, thus, the estimated values of X_n (2.22×10^4) and M_n ($= 104X_n = 2.31 \times 10^6$ g/mol) represent the upper limits of X_n and M_n, respectively. The upper limit of M_n is greater than the experimental data obtained from the polymerizations

◀

Fig. 4a, b Effect of the cosurfactant concentration on the diameter of microemulsion polymer particles. **a** C_4OH and C_4E_j and **b** C_6OH and C_6E_j

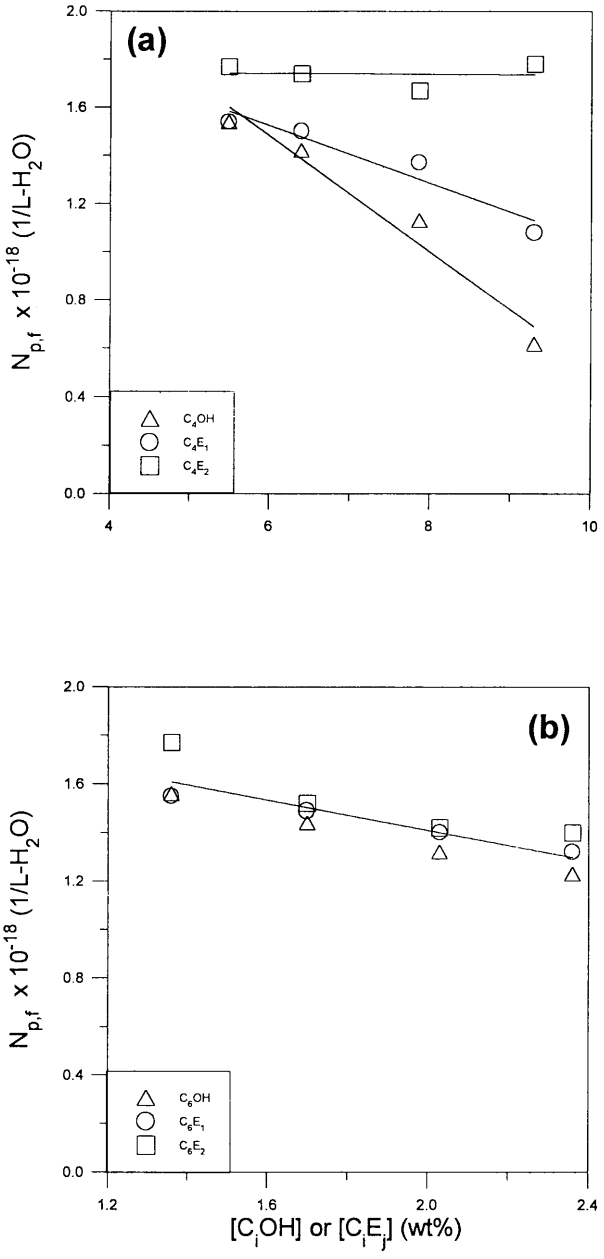

Fig. 5a, b Effect of the cosurfactant concentration on the number of microemulsion polymer particles. **a** C_4OH and C_4E_j and **b** C_6OH and C_6E_j

with various levels of C_iE_j. This result suggests that chain transfer to C_iE_j and/or bimolecular termination of free radicals belonging to two particles upon collision

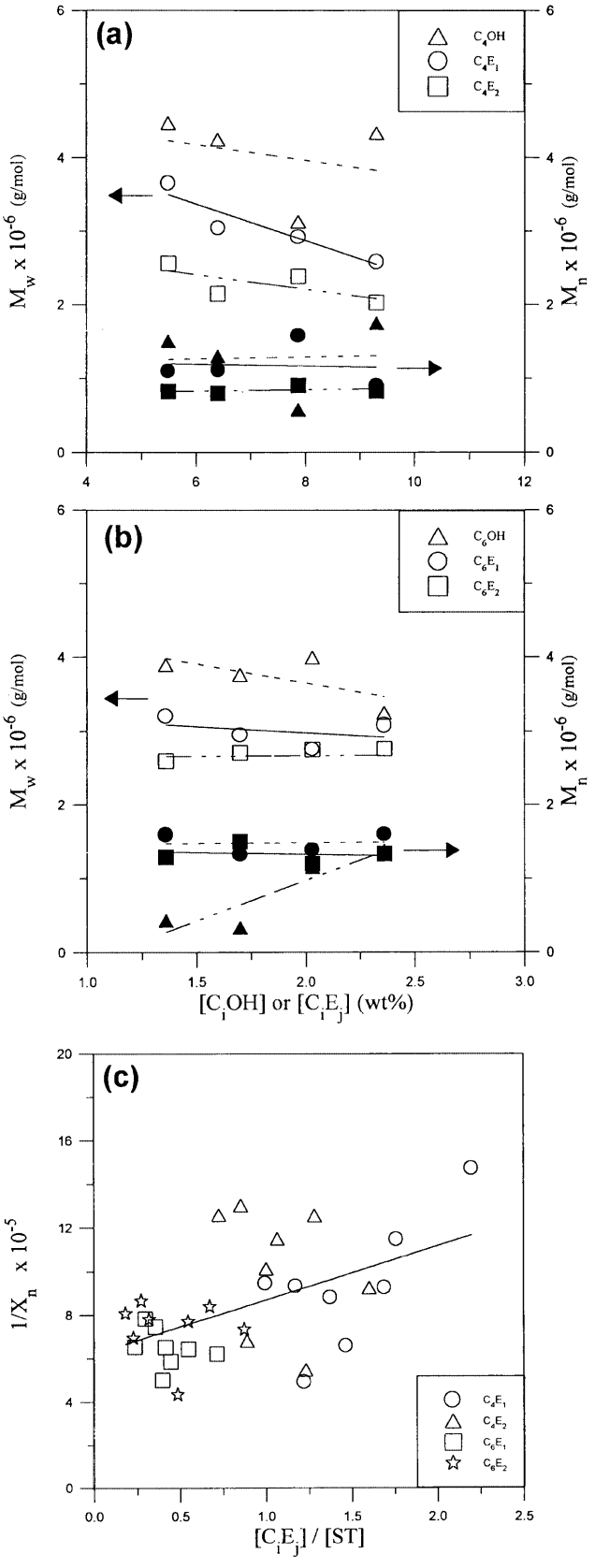

Fig. 6a, b, c Effect of the concentration of cosurfactant (**a** C_4OH and C_4E_j and **b** C_6OH and C_6E_j) on the number-average and weight-average molecular weights (*open* and *closed symbols* respectively) and **c** reciprocal of the number-average degree of polymerization as a function of [C_iE_j]/[ST]

may take place. The termination events may involve two long-chain radicals (M_n greater than the upper limit), one long-chain radical and one short-chain radical (M_n equal to or smaller than the upper limit), and two short-chain radicals (M_n much smaller than the upper limit). This scenario then results in a value of M_n equal to or smaller than the upper limit. The data of $1/X_n$ versus the ratio of the concentration of C_iE_j to the initial ST concentration are shown in Fig. 6c. Note that all the M_n data obtained from this work are included in this plot. The slope of the least-squares best-fitted straight line for the former data is the average chain transfer to C_iE_j constant (2.48×10^{-5}). The rather scattered data are attributed to the complicated polymerization mechanisms (e.g., flocculation among the interactive particles). With the d_p and M_w data, the number of PST chains per particle can be estimated (Tables 2–5). The average number of PST chains per particle is about 10, 9, 9, 6, 7

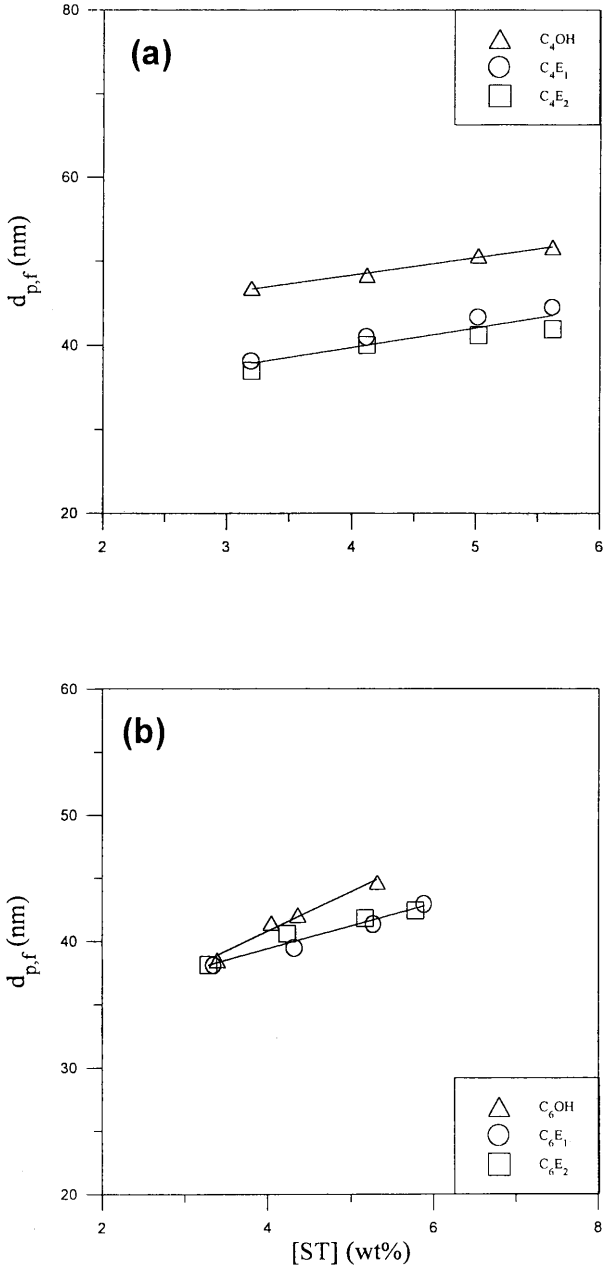

Fig. 7a, b Effect of the ST concentration on the diameter of microemulsion polymer particles. **a** C_4OH and C_4E_j and **b** C_6OH and C_6E_j

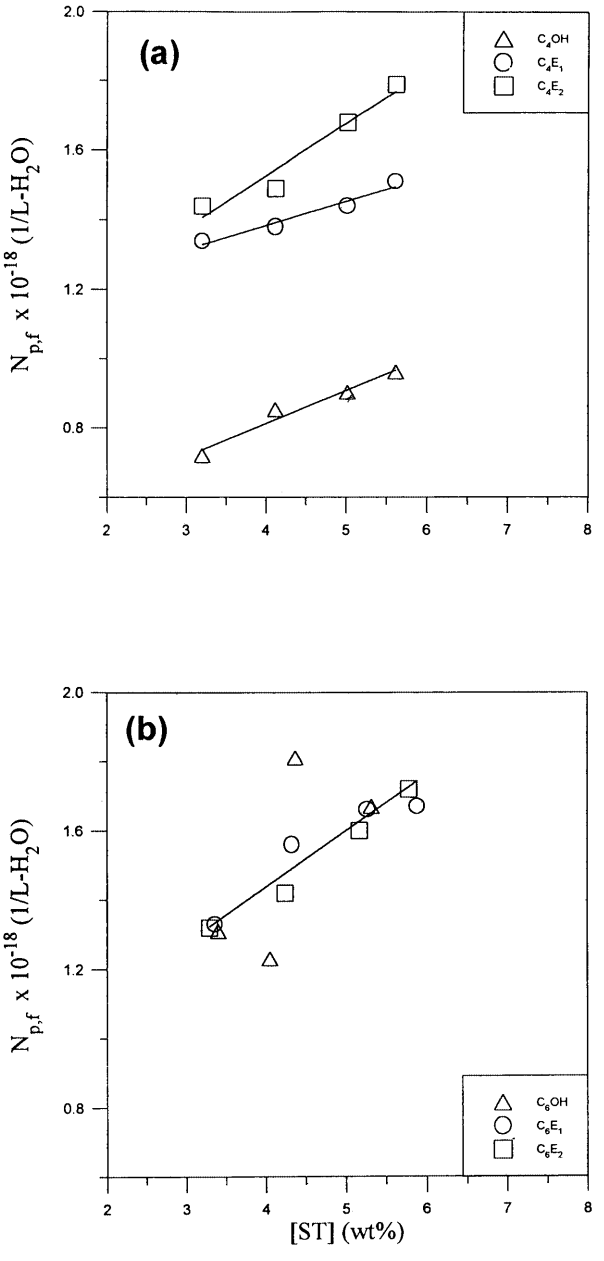

Fig. 8a, b Effect of the ST concentration on the number of microemulsion polymer particles. **a** C_4OH and C_4E_j and **b** C_6OH and C_6E_j

and 7 for the C_4OH, C_4E_1, C_4E_2, C_6OH, C_6E_1 and C_6E_2 systems, respectively. This theoretical analysis implies that, in comparison with the series of C_6OH and C_6E_j, flocculation of latex particles is more pronounced in the polymerizations with C_4OH and C_4E_j because the probability for the particles to capture more than one free radical is quite low [11].

The average d_p and $|\zeta|$ of latex particles for the C_iOH and C_iE_j systems in decreasing order is 49.4 nm and 34.7 mV (C_4OH) > 43.3 nm and 8.6 mV (C_4E_1) > 39.9 nm and 8.0 mV (C_6OH) > 39.8 nm and 7.0 mV (C_4E_2) > 38.7 nm and 6.7 mV (C_6E_2) > 39.5 nm and 3.8 mV (C_6E_1) (Ref. [11], Tables 2–5). The larger the value of d_p, the greater the absolute value of ζ. This is because the SDS concentration is kept constant at 381 mM and more SDS is available for stabilizing the larger latex particles (i.e., smaller oil–water interfacial area). As discussed previously, the SDS/C_4OH-stabilized polymerization is the least stable and limited flocculation of latex particles may occur; therefore, the aggregated particles with a higher particle surface charge density are produced in order to survive the hostile aqueous environment. It is also interesting to note that the $|\zeta|$ of the C_iE_j system is smaller than that of the C_iOH counterpart.

The recipe and some experimental results obtained from the C_iE_j-stabilized polymerizations with various concentrations of ST are compiled in Tables 2–5 (C41-3, C41-5–C41-8 in Table 2, C42-3, C42-5–C42-8 in Table 3, C61-5–C61-8 in Table 4 and C62-5–C62-8 in Table 5). The effects of ST concentration on the d_p and N_p data are shown in Figs. 7 and 8, respectively. The microemulsion comprises 25 g water, 381 mM SDS, 0.1 mM $NaHCO_3$, 1349 mM C_4OH (or 846 mM C_4E_1, 616 mM C_4E_2, 274 mM C_6OH, 274 mM C_6E_1, 336 mM C_6E_2), 0.5 mM $Na_2S_2O_8$ and various levels of ST. Both d_p and N_p increases simultaneously with increasing ST concentration because more and larger droplets are generated in the aqueous solution. It is also interesting to note that the d_p data as a function of ST concentration can be reasonably described by a single straight line for the C_iE_j systems. On the other hand, the d_p data obtained from the C_iOH system fall on a straight line which is far away from the least-squares best-fitted line for the C_iE_j systems. Figure 8a shows that, at constant ST concentration, N_p in decreasing order is $C_4E_2 > C_4E_1 > C_4OH$. On the other hand, N_p seems to be insensitive to the type of the C_6OH and C_6E_j cosurfactants used (Fig. 8b). Although the data are quite scattered, M_w seems to increase slightly with increasing ST concentration because more ST is available for the propagation reaction as the ST concentration is increased (Ref. [11], Tables 2–5). The number of PST chains per particle increases with increasing ST concentration except for the C_6E_2 series (Ref. [11], C41-3, C41-5–C41-8 in Table 2, C42-3, C42-5–C42-8 in Table 3, C61-5–C61-8 in Table 4 and C62-5–C62-8 in Table 5). The average number of PST chains per particle in decreasing order is 11.3 (C_4OH) > 9.1 (C_4E_1) > 8.5 (C_4E_2) > 7.2 (C_6E_2) > 6.9 (C_6OH) > 6.7 (C_6E_1). Again, all these results imply that the C_4OH-containing polymerization system is the least stable and that the diethylene glycol group of C_iE_j enhances the latex stability.

References

1. Prince LM (1977) In: Prince LM (ed) Microemulsions: theory and practice. Academic, New York, pp 1–20, 91–131
2. Atik SS, Thomas JK (1981) J Am Chem Soc 103:4279
3. El-Aasser MS, Lack CD, Choi YT, Min TI, Vanderhoff JW, Fowkes FM (1984) Colloids Surf 12:79
4. Johnson PL, Gulari E (1984) J Polym Sci Polym Chem Ed 22:3967
5. Jayakrishnan A, Shah DO (1984) J Polym Sci Polym Lett Ed 22:31
6. Kuo PL, Turro NJ, Tseng CM, El-Aasser MS, Vanderhoff JW (1987) Macromolecules 20:1216
7. Guo JS, El-Aasser MS, Vanderhoff JW (1989) J Polym Sci Polym Chem Ed 27:691
8. Perez-Luna VH, Puig JE, Castano VM, Rodriguez BE, Murthy AK, Kaler EW (1990) Langmuir 6:1040
9. Gan LM, Chew CH, Lye I, Imae T (1991) Polym Bull 25:193
10. Napper DH, Kim DR (1996) Macromol Rapid Commun 17:845
11. Chern CS, Liu CW Colloid Polym Sci (in press)
12. Davies JT, Rideal EK (1963) Interfacial phenomena. Academic, New York
13. Bard AJ, Faulkner LR (1980) Electrochemical methods: fundamentals and applications. Wiley, New York
14. Guo JS, El-Aasser MS, Sudol ED, Yue HJ, Vanderhoff JW (1990) J Colloid Interface Sci 140:175
15. Braks JG, Huang RYM (1978) J Appl Polym Sci 22:3111